Comparison of fracture toughness properties of advanced ferritic ODS-alloys based on 0.2T C(T) specimen tests

Charles Eiselt, David Hoelzer, Yann de Carlan, Hieronymus Hein, Marta Serrano, Pascal Diano, Herbert Schendzielorz, Andreas Seubert

COMPARISON OF FRACTURE TOUGHNESS PROPERTIES OF ADVANCED FERRITIC ODS-ALLOYS BASED ON 0.2T C(T) SPECIMEN TESTS

Charles C. Eiselt, AREVA GmbH
91052 Erlangen, Germany
Tel.: +49 9131 900-95945
Charles.Eiselt@areva.com

David T. Hoelzer, ORNL
Oak Ridge, TN 37831, USA
Tel.: +1 865 574-5096
hoelzerd@ornl.gov

Yann de Carlan, CEA
91191 Gif Sur Yvette CEDEX, France
Tel.: +33 1 69 08 6175
Yann.DeCarlan@cea.fr

Hieronymus Hein, AREVA GmbH
91052 Erlangen, Germany
Tel.: +49 9131 900-95229
Hieronymus.Hein@areva.com

Marta Serrano, CIEMAT
28040 Madrid, Spain
Tel: +34 91 3466030
Marta.Serrano@ciemat.es

Pascal Diano, AREVA NP SAS
Lyon Cedex 6, France
Tel.: + 33 472 74 8778
Pascal.Diano@areva.com

Herbert Schendzielorz, AREVA GmbH
91052 Erlangen, Germany
Tel.: +49 9131 900-95197
Herbert.Schendzielorz@areva.com

Andreas Seubert, AREVA GmbH
91052 Erlangen, Germany
Tel.: +49 9131 900-95196
Andreas.Seubert@areva.com

ABSTRACT

Based on the good experiences gained by using small specimens made of ferritic RPV materials, the Master Curve fracture toughness approach was applied to determine the fracture mechanical properties of oxide dispersion strengthened (ODS-) materials. A ferritic ODS-alloy (Fe-14Cr-1W-Ti-Y_2O_3) has been produced through the powder metallurgical production path via hot extrusion and hot isostatic pressing (HIP). Optimized oxide dispersion strengthened (ODS)-alloys have a promising potential to meet the foreseen requirements of components in future Gen IV power plants due to their high creep strength and swelling resistance under irradiation at elevated operational temperatures.
The fracture toughness was characterized with mini 0.2T C(T) specimens in different material orientations (R-L / L-R) in the ductile-brittle and upper shelf region in the un-irradiated state, accounting especially for the ODS-material's anisotropy as one key effect of manufacturing. Despite all tests were performed in orientation required by ASTM standards E 1921 and E 1820 not all validity criteria (e.g. height of yield strength, evenness of the crack, admissible K during testing or admissible stable crack growth) were met by the ODS-material: consequently, a valid T_0 value and a standard-compliant Master Curve could not be determined for the ODS-material in the transition region especially in the respective R-L orientation, also due to a comparably low fracture toughness over the whole evaluated temperature range. Promising fracture toughness properties were obtained in the crack growth direction perpendicular to the prior main deformation (extrusion) direction, where a K_{JQ} value of 196 MPa√m at T=22°C was measured. Within the ductile regime, only a $J_Q = J_{0\,2BL}$ technical initiation toughness value could be calculated and at T=22°C, a comparably large J_Q of 137kJ/m^2 is obtained for specimens with crack growth direction perpendicular to the extrusion direction, while in extrusion direction the toughness is again low.
In addition two further ODS-materials (14YWT and PM2000) were tested and compared to the alloys above. Non-conformances of ODS relating to the material requirements in ASTM standards E1921 and E1820 were finally detected and explained.

KEY WORDS

Fracture toughness, Mini 0.2T C(T) specimens, Master Curve, ODS, $K_{Jc(1T)}$, J_Q, high temperature materials

NOMENCLATURE

Δa	-	crack extension [mm]
ASME	-	American Society of Mechanical Engineers
ASTM	-	American Society for testing and Materials
C(T)	-	Compact Tension (Specimen)
HIP	-	Hot isostatic pressing
HE	-	Hot extrusion
HR	-	Hot rolling
HT	-	Heat treatment
ICM	-	Internal Conical Mandrel (test)
J	-	parameter: the difference in work per unit difference in crack area at a fixed value of displacement or, where appropriate, at a fixed value of force
J_{Ic}	-	Ductile crack initiation toughness [kJ/m^2]
$J_{0\,2BL}$	-	Technical initiation toughness [kJ/m^2]; under the respective loading a crack extension of 0.2mm through tearing occurs
J_Q	-	Ductile crack initiation toughness [kJ/m^2] unless all validity criteria are fulfilled. If all criteria are fulfilled J_Q becomes J_{Ic}
K_{Jc}	-	Static fracture toughness [MPa$\sqrt{}$m]; elastic-plastic (ASTM E1921)
$K_{Jc(1T)}$	-	Static fracture toughness [MPa$\sqrt{}$m], normalized on standard specimen thickness
$K_{Jc(med)}$	-	Equivalent value [MPa$\sqrt{}$m] of the median toughness for a multi-temperature data set
$K_{JQ(1T)}$	-	Static fracture toughness [MPa$\sqrt{}$m], normalized on standard specimen thickness (1T, 25.4 mm); calculated on the respective J_Q value
$K_{Jc(limit)}$	-	Limit value of fracture toughness [MPa$\sqrt{}$m]
L-R	-	Specimen orientation for cylindrical sections: specimen axis axial and crack propagation direction radial to main direction of forming, according ASTM E399
MA	-	Mechanical alloying
ODS	-	Oxide dispersion strengthened
ORNL	-	Oak Ridge National Laboratory
PBR	-	Powder to Ball Ratio
R_m	-	Tensile strength [MPa]
$R_{p0\,2}$	-	Yield strength [MPa]
RAF	-	Reduced activated ferritic (steels)
R-L	-	Specimen orientation: Specimen axis radial and crack propagation direction axial to main direction of forming, according to ASTM E399
PIE	-	Post Irradiation Examination
RPV	-	Reactor pressure vessel
SST	-	Small Specimen Test Technology
T	-	Temperature
T_0	-	Reference Temperature [°C], related to the temperature on the Master Curve at which the K_{Jc}=100MPa$\sqrt{}$m
T_{0Q}	-	Reference Temperature [°C], related to the temperature on the Master Curve at which the K_{Jc}=100MPa$\sqrt{}$m, unless all validity requirements are fulfilled. If all criteria are fulfilled T_{0Q} becomes T_0
W	-	Width [mm]

INTRODUCTION

An environmental friendly carbon neutral future energy scenario could involve modern Generation IV or even Fusion power plants. An important requirement for this would be the availability of suitable structural materials for high performance components within the heart of such installations like fuel claddings or first wall plates. The materials must have a set of properties, which would be high temperature strength, thermal and irradiation creep strength, resistance against (void) swelling and any structural deformation, resistance to radiation hardening / embrittlement especially during handling prior and after service [1]. This requires reasonable levels of (fracture) toughness as well. Advanced ODS materials are among a group of candidate materials, which might be able to fulfill these demands. Due to this reason, many research institutions are working on the design and characterization of according ODS-alloys [1] - [5]. However, there are still drawbacks in case of e.g. RAF-ODS steels, such as anisotropic material properties, (especially after hot extrusion), followed by a low fracture toughness in „weaker“ material orientations and lower overall workability [6]. In this context “RAF” stands for “Reduced Activated Ferritic” and means a ferritic steel with an optimized chemical composition exhibiting a lower degree of activation when used in a radioactive environment which is advantageous in terms of a final deposit after operation of the according component.

An additional point of interest is the Small Specimen Test Technique (SST), which came more into focus in the recent years [7]. The application of SST, especially for evaluation of irradiated materials, offers several advantages such as handling and treatment of smaller material amounts with fewer personal during irradiation campaigns, PIE and final storage [7]. Round robin activities for evaluation of the Master Curve approach using miniature C(T) specimens have shown, that small specimens of e.g. 4x10x10 mm dimension are suitable to produce valid T_0 reference temperatures, however, in case of RPV materials, e.g. for the Japanese SQV2A [8] - [10].

This publication addresses this ongoing topic by connecting the advanced material class of ODS alloys with the SST approach. Mechanical-technological investigations with a focus on fracture toughness were performed upon four ODS-materials obtained from different institutions. In addition the applicability of the current ASTM standards E 1921 and E 1820 in combination with ODS has been cross checked.

MATERIALS AND SPECIMENS

Within this study four ODS materials are being evaluated. At first a RAF-ODS-material was produced by the powder-metallurgical route by mechanical alloying of a 10kg pre-alloyed Fe-14Cr-1W-0.3Mn-0.3Si-0.25Ti steel powder and 0.25% nanosized Y_2O_3 + TiH_2 powder by the external supplier Zoz GmbH within the large scale CM100b mill. The milling balls used in the process were made of 100Cr6. The milling

time was selected to be 12h with a PBR of 1:10 at intervals of 316rpm/4min to 211rpm/1min under a reducing H_2 milling atmosphere. Before and after the milling run at unloading the chamber atmosphere was changed into inert Ar gas. Furthermore the milled powder was compacted via the two different processes hot extrusion and HIP. For hot extrusion the powder was filled in a stainless steel canister, degassed at 400°C for 2h and directly hot extruded at T=1100°C into an ODS-material rod, exhibiting a final outer diameter of 20mm and length of ~2m. This alloy is designated as S1. For HIP the powder was loaded in canisters, degassed and hipped into slabs at 1050°C, 1400bar for 4h (material designation S2). Finally a heat treatment of 1050°C for 1h was carried out on both ODS materials for stress relief and for establishment of identical final material conditions.

A further ODS-material being investigated was the ORNL developed 14YWT [11] [12]. Earlier studies have revealed, that certain heats of this alloy had superior strength and fracture toughness properties [11] [12]. A new 14YWT heat was produced with existing pre-alloyed Fe-14Cr-3W-0.4Ti and 0.3% Y_2O_3 powder, also by mechanical alloying 5.4kg of powder in 6 batches using a Zoz CM08 attritor mill. In addition the milled powder was filled in 3 mild steel cans which were degassed at 300°C for 24h and extruded at 850°C into rectangular shaped bars. The extruded bars were cut into smaller sections and were hot rolled normal to the extrusion directions into several plates at 1000°C. The alloy is designated as S3.

Finally data of another commercial ODS material, the PLANSEE manufactured PM2000 (alloy S4), is part of this study for the purpose of comparison [13]. The material was obtained in the hot rolled state. The chemical compositions of the evaluated ODS materials can be seen in **Table 1**:

	C	Cr	W	Ti	Si	Ni	Mn	Al	Y_2O_3
S1	0.047	13.9	1.09	0.25	0.31	0.22	0.34	0.011	0.20
S2	0.015	14.0	1.11	0.23	0.30	0.20	0.34	<0.01	0.22
S3	0.024	14.3	2.32	0.27	0.04	0.012	0.008	0.016	0.30
S4	n/a	19.0	n/a	0.50	n/a	n/a	n/a	5.50	0.50

Table 1: **Chemical compositions [wt.%] of the ODS-alloys S1-S4** [13]

The available S1-S4 material pieces available for investigations in this study are summarized in **Figure 1** a)-d). In case of the S1 alloy the application of the SST allowed a machining of 0.2T C(T) mini fracture toughness specimens in extrusion (R-L) and perpendicular (L-R) direction, which is displayed in **Figure 2** a) and b). Through this measure a direct analysis of the toughness properties in both orientations was possible. For the hipped S2 material no predominant orientation existed and the 0.2T C(T) mini fracture toughness specimens were extracted out of the hipped slab as most appropriate. For S3 the 0.2T C(T) mini fracture toughness specimens were machined in the characteristic plate orientation E-R, resulting from the hot rolling process during S3 manufacture (see **Figure 1** c)) and **Figure 2** c)). For S4, the 0.2T C(T) mini fracture toughness specimens used in this study were taken in T-L orientation of the block (**Figure 1** d)) and **Figure 2** d)), resulting from the rolling direction as well. In

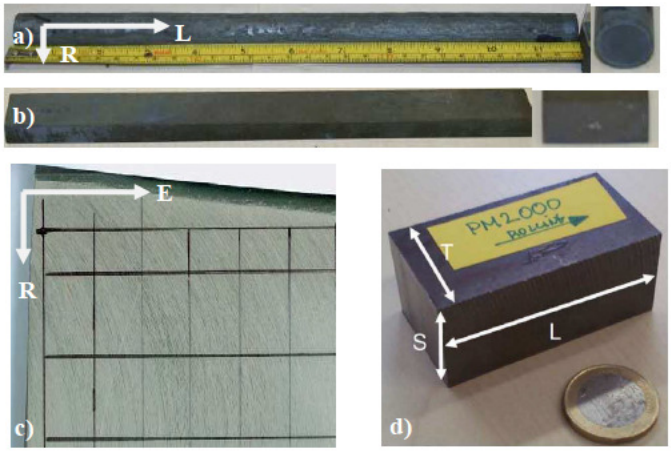

Figure 1: **ODS materials available for investigations; a) hot extruded S1 rod, b) hipped S2 slab, c) hot rolled S3 plate, d) hot rolled S4 block**

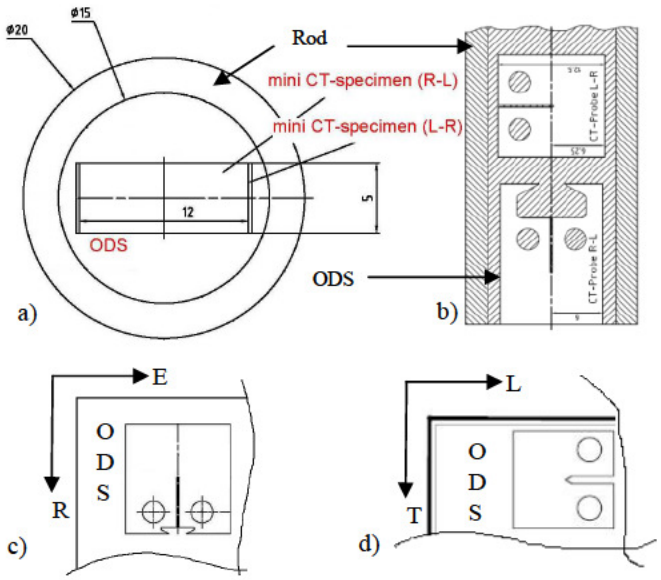

Figure 2: **Specimen take out positions: a), b) S1 in R-L and L-R orientation, c) S3 in E-R orientation, d) S4 in T-L orientation**

Figure 3 a)-c) the applied 0.2T C(T) specimen geometries used in this study are shown. For an improved test execution „measuring edges" were attached to the C(T)-5 specimens in an earlier design (see **Figure 3** a)). **Table 2** gives an overview of the investigated materials, specimens and tests.

FRACTURE TOUGHNESS TEST PROCEDURES

All fracture toughness tests were conducted using the mini specimens shown in the previous chapter and through application of the unloading compliance technique.

Prior to testing all 0.2T C(T) specimens were fatigue pre-cracked through a high frequency vibration load in such a way, that the crack had an average final length of a_0=5mm (± 0,5mm) leading to a ratio of 0,5 (± 0,05) between the specimens' width W and a_0. The crack propagation was hereby visually controlled. For the 0.2T C(T) specimens tested according to the standard ASTM E 1921-13 3 specimens of S1 R-L and 2 specimens of S2 slightly exceeded the admissible stress intensity factor at the end of pre-cracking [14]. For the 0.2T C(T) specimens tested according to the standard ASTM E 1820-11 the maximum load P_{max} to be kept during pre-cracking procedure was never exceeded [15].
Due to the very small specimen geometry a correction towards the loadline had to be made for **Figure 3** a), b) and c) specimens. The calculated compliance was integrated in the test evaluation [16].

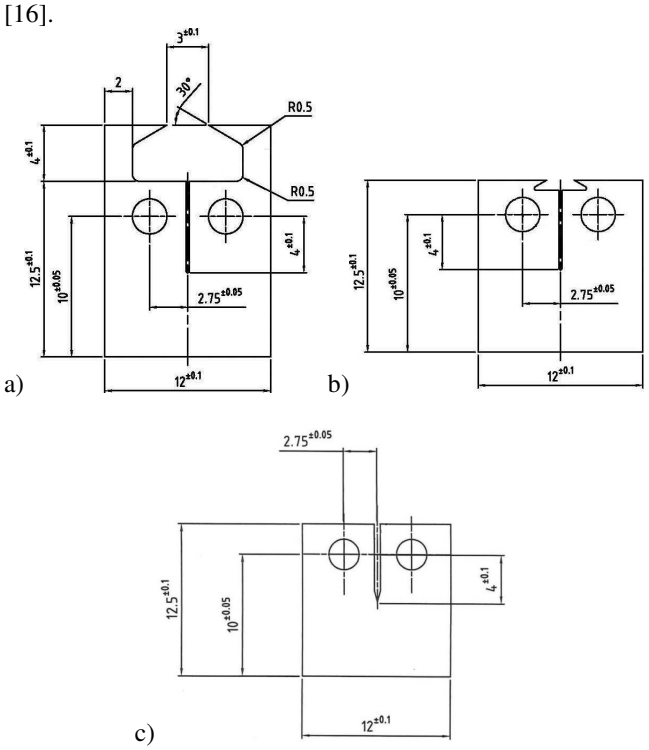

Figure 3: **0.2T C(T) mini fracture toughness specimen geometries used in the study: a) with measuring edges, b), c) no edges**

Material ID	S1	S2	S3	S4
Material type	Fe-14Cr + Y_2O_3	Fe-14Cr + Y_2O_3	Fe-14Cr + Y_2O_3	Fe-19Cr + Y_2O_3
Manufacturing process	MA + HE + HT	MA + HIP + HT	MA + HE + HR	MA + HE + HR
Specimen type	0.2 T C(T)	0.2 T C(T)	0.2 T C(T)	0.2 T C(T)
Orientation	R-L / L-R	-	E-R	T-L
Types of tests following the standard	ASTM E 1921 and E 1820	ASTM E 1921 and E 1820	ASTM E 1921	ASTM E 1820

Table 2: **0.2T C(T) mini fracture toughness specimen geometries used in the study: a) with measuring edges, b), c) no edges**

One part of the tests was performed in the brittle-/ductile transition regime: for the tests with S1, S2 and S3 materials the elasto-plastic test was performed using an Instron type 5569 class1 ball screw testing device, the suitability of the clip gage was approved with DIN EN ISO 9513 [17].
The temperature close to the specimens was measured by two calibrated thermocouples. Following the ASTM E 1921-13, which served as an orientation in this study by taking into account its validity criteria, a $K_{Jc(1T)}$ [MPa√m] value in dependence of test temperature was determined [14].
The materials tested in the transition regime were S1, S2 and S3. The chosen test temperatures for S1 and S2 were in a span of -100°C ≤ T ≤ 125°C and in case of S3 in an area of -150°C≤ T ≤ 22°C.
A further part of the fracture toughness tests was executed in the ductile upper shelf regime as J-Δa tests following the standard ASTM E 1820-11, to obtain firstly the ODS crack resistance curves with the final objective to calculate a respective J_{Ic} value, in case the according validity criteria can be met [15]. For S1 5 specimens were tested in L-R at T=22°C and 3 tests were performed in R-L orientation at 125°C. For S2 6 tests were performed at T=300°C and S4 was tested with 3 specimens at 0°C. Some of the higher test temperatures were used to calculate the respective $K_{JQ(1T)}$ value based on the measured J_Q data according to [14].
In order to calculate the characteristic fracture toughness values of the alloys, according tensile data (not mentioned here) were used. In this context the tensile data obtained for the S1 alloy and subsequently applied for S1 fracture toughness evaluation was used for the S2 fracture toughness evaluation as well because the material composition of S1 and S2 is the same and no direct S2 tensile data was available. In case of S3 the according tensile data were taken from an earlier heat (SM12) with a similar composition as S3. In case of S4 available tensile information was applied.

TEST RESULTS

Figure 4 contains a comparison of the characteristic $K_{Jc(1T)}$ and $K_{JQ(1T)}$ values obtained from the investigated ODS S1, S2 and S3 materials. In case of S1, the SST technique allowed the analyses of orientation effects on the fracture toughness properties by testing 0.2T C(T) specimens in R-L and L-R directions as shown in **Figure 2**. In the T-range between -100°C ≤ T ≤ -50°C $K_{Jc(1T)}$ lies in between 35.7 MPa√m and 54.9MPa√m for ODS01 L-R. Then, after entering the sharp transition regime $K_{Jc(1T)}$ strongly increases up to 85.7MPa√m at T=0°C and then up to a $K_{JQ(1T)}$ of 196.2 MPa√m at T=22°C. For S1 R-L $K_{Jc(1T)}$ is a lot lower in between -100°C ≤ T≤ -50°C, by staying around 26 MPa√m. In contrast to the L-R orientation no increase of $K_{Jc(1T)}$ and $K_{JQ(1T)}$ is detected up to T=125°C. The highest value of the test series is 41 MPa√m at T=50°C. $K_{Jc(1T)}$ of the S2 alloy exhibits at first a little higher level then obtained in the R-L direction of S1 which is 52.0 MPa√m at

T=-50°C and 54.5 MPa√m at T=0°C. However, at temperatures between 50°C and 300°C $K_{Jc(1T)}/K_{JQ(1T)}$ remain almost constant at a comparably lower level of max 39.9 MPa√m (at 100°C). Overall the S3 E-R alloy seems to have the highest fracture toughness of the three ODS-alloys, at least up to 0°C: starting at an intial $K_{Jc(1T)}$ of 32.2 MPa√m at -150°C a slight increase up to 48.5 MPa√m at -100°C is detected with practically two identical measurements at this temperature, indicating a lower degree of scattering (see **Figure 4**). This behavior changes at T=-75°C with two higher $K_{Jc(1T)}$ measurements of 71.8 MPa√m and 108.2 MPa√m, which is the largest value reached for S3, resulting in higher scattering effects. Neither S1 L-R /R-L nor S2 rises to such toughness levels at this temperature, in case of S1 L-R the increase begins at T=-25°C with a $K_{Jc(1T)}$ value of 63.5 MPa√m. At -60°C S3 shows a reduced fracture toughness of 46.7 MPa√m, while afterwards rising again to 71.0 MPa√m at -50°C. This stands for some sort of scattering behavior as well. At room temperature S3 E-R reaches a final value of 90.6 MPa√m, which is quite close to 85.7 MPa√m at T=0°C. However, the $K_{JQ(1T)}$ of 196.2 MPa√m of S1 L-R at RT is not reached.

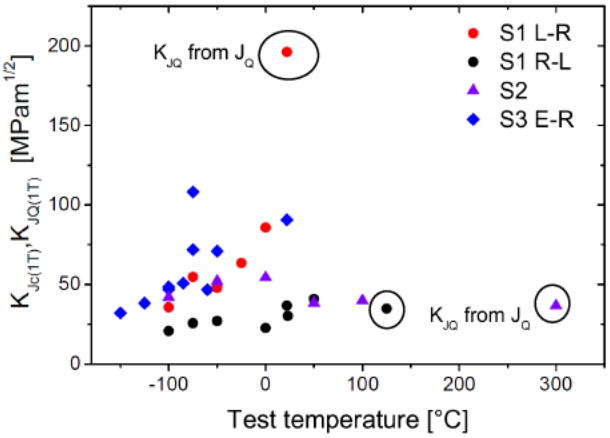

Figure 4: **Fracture toughness $K_{Jc(1T)}$, $K_{JQ(1T)}$ data in the transition region of S1, S2, S3 ODS-materials**

Since the ASTM Standard E 1921-13 [14] serves as an orientation for the fracture toughness tests, an important objective is to determine a Master Curve and an according T_0 or T_{0Q} value, where feasible, to have these characteristic fracture toughness values available also for ODS-materials based on mini 0.2T C(T) specimens in order to address future regulators requests. This has been tried for S1 L-R in **Figure 5** and S3 E-R in **Figure 6**.

In case of S1 L-R 6 data points are used to calculate the Master Curve according to [14]. The very high $K_{JQ(1T)}$ value of 196.2 MPa√m at T=22°C is not taken into consideration, because it is far beyond the allowable 98% confidence bounds. The data point of 54.8 MPa√m at T=-75°C (being slightly below the 98% boundary curve) is still part of the analyses. Despite none of the tested specimens actually reached the required 100 MPa√m for a T_0 it was possible to draw the Master Curve for S1 L-R. This lead to a T_{0Q} of ~13.5°C at 100 MPa√m, which is however not valid, because validity criteria of ASTM E 1921-13 could not be met: specimens out of the fixed T_0 +/- 50°C range were used.

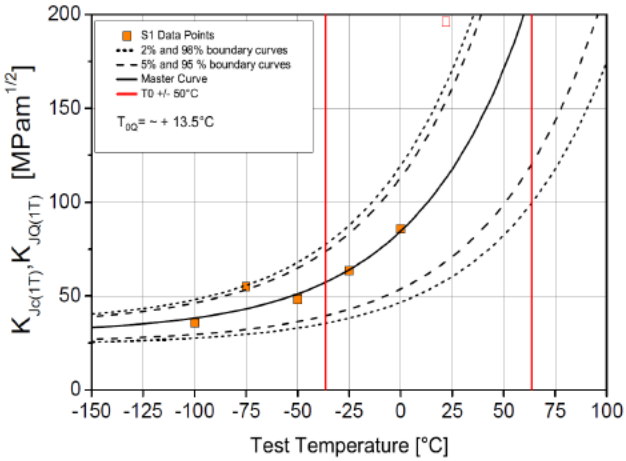

Figure 5: **Master Curve and T_{0Q} determination for S1 L-R**

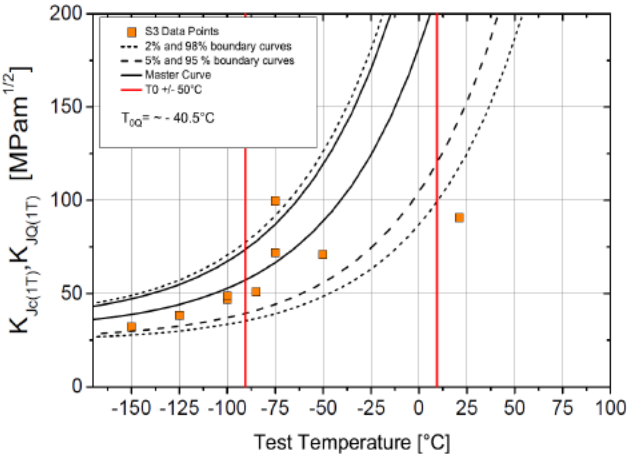

Figure 6: **Master Curve and T_{0Q} determination for S3 E-R**

This was done because it was necessary to study the fracture toughness development in the lower shelf and to determine the beginning of the transition region. More specimens were not available at this time but this point might be solved in future test campaigns and it is assumed that the obtained T_{0Q} will not change much. In addition the material's yield stress exceeds 825MPa. A similar approach was done for S3 E-R (see **Figure 6**). In this case also all available specimens were used to calculate the Master Curve, despite the T_0 +/- 50°C range criteria could not be met and two specimens were out of the 2% and 98% confidence bounds. In addition for some (not for all) of the specimens the criteria maximum difference between initial crack length a_0 and crack lengths a_{01} to a_{09} (see [14]) was exceeded. Furthermore the specimen at T=-50°C ($K_{Jc(1T)}$=71.0 MPa√m) had a very uneven crack growth during pre-cracking.

Despite these difficulties a T_{0Q} of -40.5 °C was obtained for S3 E-R. A higher test amount of further specimens in the allowable range might further refine that result.

Due to the promising increase of S1 L-R $K_{Jc(1T)}$ in the transition regime it was decided to perform some more J-da tests at T=22°C, normally conducted in the ductile upper shelf regime, with an orientation on ASTM E 1820-11 [15]. In addition, data for S1 R-L at T=125°C, for S2 at 300°C and for S4 at T=0°C were available for comparison. The according J-da diagram is shown in **Figure 7**.

Since the ASTM E 1820 validity criteria "admissible stable crack growth" was not met for some specimens of all tested materials no final J_{Ic} value could be calculated. However, in this case ASTM E 1820-11 allows a determination of a $J_Q = J_{0.2BL}$ technical initiation toughness value as a fracture toughness measurement instead, representing the J-value at a crack extension of 0.2mm, calculated from several specimens at one specific temperature through application of the multi-specimen test technique.

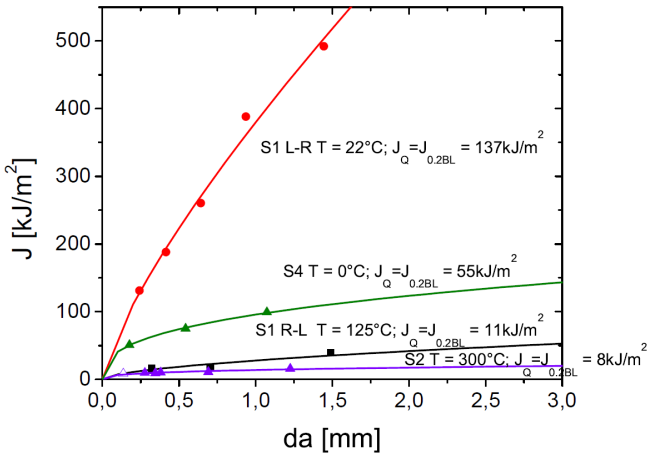

Figure 7: Fracture toughness J and $J_Q = J_{0.2BL}$ data in the upper shelf region of S1, S2, S4 ODS-materials

The strength difference between the two investigated L-R/R-L orientations for S1 and in addition S2 becomes even more distinct: At T=22°C, a comparably very large J_Q for S1 L-R of 137kJ/m² is observed together with a rather steep rise of the J-da curve. Despite the increased test temperature of T=125°C, where a higher degree of ductility is normally expected, J_Q exhibits only a comparably very low value of 11kJ/m² for S1 R-L. In case of S2, at a higher test temperature of T=300°C, the result tends even more downwards with 8kJ/m². The slope of both J-da curves is rather flat. Therefore the probability for unstable brittle fracture is a lot larger for S1 R-L and S2 than for S1 L-R at the tested temperatures. The S4 J_Q value of 55kJ/m² tested at T=0°C, also a lower test-temperature, lies in between the levels for the other materials. However since this S4 ODS-material behaves in a more ductile way, it is assumed, that its J_Q levels will be more close to S1 L-R at higher test temperatures.

DISCUSSION

The observed differences in the fracture toughness of the ODS-materials investigated can be principally attributed to the selected manufacturing processes. For example hot extrusion of a ferritic ODS rod produces an elongated grain structure and a texture in extrusion direction as shown in earlier investigations [1]. The strong increase of S1 $K_{Jc(1T)}$ in L-R orientation within the transition region, especially at T=22°C, results from this anisotropy in the microstructure: a crack with crack growth direction perpendicular to the extrusion direction requires a lot more energy to be propagated and in this context even crack bifurcation (turning of the crack propagation plane in extrusion direction) might occur. On the contrary, when the crack is orientated in extrusion direction, it can easily grow along the grain boundaries encountering a low material resistance against this propagation due to smaller grain boundary cohesion forces, which leads finally to the measured lower fracture toughness in R-L orientation of S1. However, a larger number of tests is required to check for scattering effects. Since S2 does not have a predominant texture caused by manufacturing by HIP, it does not profit from a toughness increase. In the transition regime it shows slightly larger $K_{Jc(1T)}$ values at T=-50°C and T=0°C than S1 R-L coming close to S1 L-R but already at 0°C the S1 L-R levels are not reached anymore, in fact at higher temperatures S2 behaves in a similar way to the low toughness regime of S1 R-L. This underlines again the need for further thermomechanical treatment (e.g. hot rolling) for hipped ODS materials, which was not part of this study.

The slightly better performance of S3 E-R compared to S1 L-R up to T=-50°C might as well be a result of a more optimized thermomechanical (hot rolling) process (e.g. a higher degree of deformation). However, it is observed, the material scatters quite strongly in between -75°C ≤ T ≤ -50°C, which could be caused by microstructural inhomogeneities in the final material. Another explanation, relating to other S3 heats and more in context of high temperature fracture toughness, is given here [18]: a higher alloy purity, meaning a reduced content of N and O with lower segregation levels on the grain boundaries leading to stronger cohesion forces between the grains could significantly improve the fracture toughness. Exact comparable data for S1 (and for S2) are currently not available and it remains in question, whether a higher purity could improve the fracture toughness of S1 in the transition regime but this point could play a role. The difference between S1 L-R and S3 E-R at T=22°C ($\Delta K_{Jc(1T)}/\Delta K_{Q(1T)}$= ~105.6 MPa√m) is quite striking, but here more tests at this and also higher temperatures are necessary to analyse the behaviour in detail.

The J-da tests reveal a similar behaviour: the low toughness of S1R-L and S2 as a consequence of the assumed production impacts on the microstructure is maintained up to T=300°C, since no improvement of J_Q is detected. In this study S1 L-R shows a high J_Q (137kJ/m²) at T=22°C but further test campaigns have to reveal how it performs at operating fast reactor plant temperatures (T~550°C and beyond). The better ductility of S4 already at

T=0°C might be a consequence of the hot rolling technique used during production as well.

It has to be stated, that "thick" materials have been investigated in this study. A later cladding tube as a "thin-wall" component will encounter more significant deformations through application of additional production steps like cold pilgering and/or cold drawing after hot extrusion (not done in this study) in order to obtain the final dimension of the component. Therefore it is assumed, that e.g. a full S1 ODS-cladding might probably exhibit even higher toughness levels, than determined in this investigation. Other very recent test campaigns (ICM tests) done on real ferritic ODS-claddings with a crack propagation in R-L orientation reveal fracture toughness values close to ~160MPa√m at room temperature [19].

However, the increasing tendency of the fracture toughness for S1 L-R and S3 E-R in the transition regime allowed the determination of a Master Curve and an according T_{0Q} based on SST tests with 0.2T C(T) specimens, which on the contrary was not feasible for S1 R-L and S2 because the fracture toughness remained low. However, despite successful tests, several important validity criteria, as summarized in **Table 3** and **Table 4**, could not be met in the transition and upper shelf regime. It has also to be added that the yield stress of optimized ODS alloys with ($R_{p0\,2} \geq$ 1000MPa at T=22°C) [1] [18] is already too high compared to the range of more "conventional" ferritic steels' yield stresses (275 to 825 MPa) covered by [14], which is further reason for their non-conformance to [14]. For now, these findings lead to invalid T_{0Q} or J_Q characteristic values.

For a valid T_0 the test temperatures should be selected close to that at which $K_{Jc(med)}$ reaches the 100 MPa√m [14] . Despite it is not an explicit demand of the ASTM E 1921-13, it is recommended that at least some of tested specimens actually reach the 100 MPa√m, in order to have this as a stronger confirmation of the determined T_0 value. If this is not the case, the uncertainty of the T_0 value is increased, which would result in the necessity to test a higher number of specimens to again reduce this uncertainty. The $K_{Jc(limit)}$ was far from being reached during all tests, therefore it is assumed, that 100 MPa√m can be reached with 0.2T(CT) specimens. When not considering the ASTM E 1921-13 yield stress requirements, testing more specimens in this temperature range might eventually lead to a more refined and "nearly valid" T_0, at least for S1 L-R.

Nevertheless, the invalid results seem to be a matter more of ODS materials' non-conformance to standards then of SST and the application of 0.2T C(T) mini specimens in general. This is underlined by other investigations [8] - [10] were valid and consistent T_0 transition temperatures were determined for ferritic RPV steels. Therefore mini-C(T) specimens seem principally suitable to be applied for fracture toughness investigations of structural materials offering many advantages especially when dealing with irradiated materials. Future test campaigns will involve more high temperature testing of ODS materials in the operating temperature regime of e.g. Fast Reactors.

Material	T_{0Q} [°C]	validity criteria unmet*
S1 L-R	13.5	- Tests out of T_0 +/- 50°C range - Yield stress exceeds 825 MPa
S1 R-L	-	- 3x specimens slightly exceeded the admissible stress intensity factor at pre-cracking - No increase of fracture toughness - Yield stress exceeds 825 MPa
S2	-	- 2x specimens slightly exceeded the admissible stress intensity factor at pre-cracking - No increase of fracture toughness - Yield stress exceeds 825 MPa
S3	-40.5	- Tests out of T_0 +/- 50°C range - Maximum difference between initial crack length a_0 and crack lengths a_{01} to a_{09} exceeded - Yield stress exceeds 825 MPa
*according to ASTM E 1921-13		

Table 3: T_{0Q} and unmet validity criteria for the investigated ODS-materials in the transition regime according to ASTM E 1921-13 [14]

Material	Test T [°C]	$J_Q = J_{0.2BL}$ [kJ/m²]	validity criteria unmet*
S1 L-R	22	137	maximum of stable crack growth extended
S1 R-L	125	11	maximum of stable crack growth extended, insufficient number of tests
S2	300	8	maximum of stable crack growth extended
S4	0	55	maximum of stable crack growth extended, insufficient number of tests
* according to ASTM E 1820-11			

Table 4: J_Q and unmet validity criteria for the investigated ODS-materials in the upper shelf regime according to ASTM E 1820-11 [15]

In addition a future adaption of according standards in order to better cover the specific ODS high strength behavior together with a standardization of ODS-production (if feasible) will be a future task to provide the necessary characteristic material properties by fully valid material tests to address regulators and operators safety requests.

SUMMARY AND CONCLUSIONS

This study aims in connecting fracture toughness investigations in the transition and upper shelf regime based on mini 0.2T C(T) specimens with the class of high strength ODS materials, being a candidate for future high temperature applications in Fast Reactors or Fusion Power Plants. In this context four ODS-materials were analyzed by mechanical testing and following conclusions can be made:

- Fracture toughness tests of ODS with 0.2T C(T) were successfully conducted up to 300°C.
- Several validity criteria of ASTM E 1820-11 and 1921-13 could not be met, but this seems to be more a matter of ODS materials' non-conformance than of SST based on 0.2T C(T) tests.

- Despite final invalid T_{0Q} and J_Q data were obtained, mini C(T) specimens are principally suitable for valid T_0 determination and to be used in fracture toughness analyses as other studies on ferritic RPV have shown.
- Master Curves were successfully obtained for S1 L-R and S3 E-R.
- The alloy S3 E-R exhibits slightly higher $K_{Jc(1T)}$ levels than S1 L-R in the transition region up to 0°C, while S1 L-R exhibits a very high $K_{Jc(1T)}$ of 196.2 MPa√m at 22°C; also in the upper shelf regime S1 L-R shows a high J_Q of 137kJ/m^2 at T=22°C with S4 exhibiting a J_Q of 55kJ/m^2 at T=0°C; the highest fracture toughness was obtained for hot extruded ODS-material specimens with a crack growth direction perpendicular to the extrusion direction.
- The alloys S1 R-L and S2 exhibit low fracture toughness levels over the whole tested temperature regime; therefore no characteristic T_{0Q} and MC could be obtained.
- The anisotropic fracture toughness properties of S1 L-R/R-L in general as well as the good overall performance of S1 L-R, S3 E-R and the lower toughness levels of S1 R-L and S2 in the investigated temperature regimes are attributed to the different applied production paths, respectively to hot extrusion and hot rolling as well as to the alloys' impurity levels (N,O).
- Execution of a full thin walled cladding manufacture might lead to even higher (fracture) toughness levels for e.g. a S1-ODS-cladding through increased deformations introduced by additional production steps (e.g. cold pilgering); very recent ICM tests on other ferritic ODS-claddings already prove this assumption with R-L fracture toughness levels of ~160MPa√m at room temperature.

Based on the promising results and experiences obtained in this study the SST approach will be systematically continued: next steps will address higher temperature regimes (550°C ≤ T ≤ 800°C). The study will include different ODS-alloy types and RPV materials. Later on an inclusion of irradiated materials as well as tests on real cladding tubes might round these characterization efforts.

ACKNOWLEDGMENTS

We thank all partners who contributed to this effort in various manners: parts of the results in this study were obtained within an IAEA CRP-T11006 on ODS. In this context a part of the mini fracture toughness 0.2T C(T) specimens were machined by HZDR Rossendorf (Dr. Altstadt, Dr. Viehrig) with support of KIT (Mr. Lindau). The ODS material S3 was provided by ORNL (Dr. Hoelzer) and S4 by CIEMAT (Dr. Serrano). Beyond this activity the S1, S2 materials were mechanically alloyed in Zoz GmbH, hot extruded in CEA (Dr. Sornin) and hipped in AREVA SAS Technical Center France (Dr. Cedat). The fracture toughness tests were performed in AREVA GmbH Technical Center Germany (Mr. Schendzielorz, Mr. Seubert). We thank all main contributors/ partners, especially AREVA NP SAS SFR project (Mr. Diano, Mr. Hamy) and AREVA GmbH (Dr. Eiselt, Mr. Hein) for their continued cooperation and support of AREVA's ODS activities, making this overall study possible on a global scale.

REFERENCES

[1] Rouffié, A.L., Wident, P., Ziolek, L. et al., Influence of process parameters and microstructure on the fracture mechanisms of ODS steels, Journal of Nuclear Materials 433 (2013) 108 – 115

[2] Eiselt, C.C., Klimenkov, M., R. Lindau, Möslang, A., Characteristic results and prospects oft he 13Cr-1W-0.3Ti-0.3Y_2O_3 ODS steel, Journal of Nuclear Materials 386-388 (2009) 525 – 528

[3] McClintock D.A., Hoelzer, D.T., Sokolov, M.A., Nanstad, R.K., Mechanical properties of neutron irradiated nanostructured ferritic alloy 14YWT, Journal of Nuclear Materials 386-388 (2009) 307 – 311

[4] de Carlan, Y., Bechade, J.-L., Dubuisson, P., et al., CEA developments of new ferritic ODS alloys for nuclear applications, Journal of Nuclear Materials 386 – 388 (2009) 430 - 432

[5] Byun, T.S., Yoon, J.H., Hoelzer, D.T., Lee, Y.B. et al., Process development for 9Cr nanostructured ferritic alloy (NFA) with high fracture toughness, Journal of Nuclear Materials 449 (2014) 290 – 299

[6] Chaouadi, R., Ramesh, M., Gavrilov, S., Effect of crack length-to-width ratio on crack resistance of high Cr-ODS steels at high temperature for fuel cladding application, Journal of Nuclear Materials 442 (2013) 425 – 433

[7] Sokolov, M., Nanstad, R., Use of small specimens for fracture toughness characterization of fracture toughness of irradiated materials, SMIRT-22 Transactions Division II, San Francisco, California, USA, August 18-23, 2013

[8] Yamamoto, M., Kimura, A., Miura, N. et al., A round robin program of Master Curve evaluation using miniature C(T) specimens: first round robin test on uniform specimens of Reactor Pressure Vessel Material, Proceedings of the ASME 2012 PVP, July 15-19, 2012, Toronto, Ontario, Canada.

[9] Yamamoto, M., Miura, N. et al., A round robin program of Master Curve evaluation using miniature C(T) specimens -2nd report: fracture toughness comparison in specified loading rate condition-, Proceedings of the ASME 2013 PVP, July 14-18, 2013, Paris, France

[10] Yamamoto, M., Kimura, A., Miura, N. et al., A round robin program of Master Curve evaluation using miniature C(T) specimens -3rd report: comparison of T_0 under various selections of temperature conditions-, Proceedings of the ASME 2014 PVP, July 20-24, 2014, Anaheim, California, USA

[11] McClintock, D.A., Sokolov, M.A., Hoelzer, D.T., Nanstad, R.K., Mechanical properties of irradiated ODS-Eurofer and nanocluster strengthened 14YWT, Journal of Nuclear Materials 392 (2009) 353 - 359

[12] McClintock, D.A., Hoelzer, D.T., Sokolov, M.A., Nanstad, R.K., Mechanical properties of neutron irradiated nanostructured ferritic alloy 14YWT, Journal of Nuclear Materials 386 - 388 (2009) 307 - 311

[13] Garcia-Juceda, A., Rodriguez, D., Serrano, M., Influencia del Envejecimiento en las Propriades Mecánicas de un acero ODS, XII Congreso Nacional de Materiales-IBEROMAT, Alicante, 30th May -1st June, 2012, 4 p.

[14] Standard Test Method for Determination of Reference Temperature T_0, for Ferritic Steels in the Transition Range ASTM E 1921-13

[15] Standard Test Method for Measurement of Fracture Toughness ASTM E 1820-11

[16] Saxena, A., Hudak, S.J., Review and Extension of Compliance Information Crack Growth Specimens, International Journal of Fracture, Vol.14, No.5 (1978)

[17] DIN EN ISO 9513, Metallic materials – Calibration of extensometer used in uniaxial testing, May 2013

[18] D.T. Hoelzer, et al., Influence of processing on the microstructure and mechanical properties of 14YWT, Journalof Nuclear Materials (2015) http://dx.doi.org/10.1016/j.jnucmat.2015.12.011

[19] Carlan, Y.de, private communication, 29.02.16